JACS
JOURNAL OF THE AMERICAN CHEMICAL SOCIETY

COMMUNICATION

pubs.acs.org/JACS

Nanopatterning by Molecular Polygons

Stefan-S. Jester,* Eva Sigmund, and Sigurd Höger*

Kekulé-Institut für Organische Chemie und Biochemie, Rheinische Friedrich-Wilhelms-Universität Bonn, Gerhard-Domagk-Strasse 1, 53121 Bonn, Germany

Supporting Information

ABSTRACT: Molecular polygons with three to six sides and binary mixtures thereof form long-range ordered patterns at the TCB/HOPG interface. This includes also the 2D crystallization of pentagons. The results provide an insight into how the symmetry of molecules is translated into periodic structures.

The adsorption of rigid (conjugated) oligomers on solid surfaces is an effective way to produce long-range ordered two-dimensional nanoscale functional arrays.[1] To ensure sufficient compound solubility—necessary to isolate, purify and characterize the final target structures and their precursors—alkyl chains are attached to the molecular backbones. Moreover, linear alkyl chains drive the molecule physisorption onto the substrate, and link the adsorbates by side chain interdigitation.[2,3] A powerful tool for the investigation of monolayers on solid surfaces is scanning tunneling microscopy (STM), often performed *in situ* at the liquid/solid interface using 1,2,4-trichlorobenzene (TCB) as solvent and highly ordered pyrolytic graphite (HOPG) as substrate. Surface regions covered with backbones and crystallized alkoxy substituents appear in bright and dark color, representing high and low tunneling efficiencies, respectively.[4,5]

Within the past decade, considerable effort has been given to explore the design rules for the creation of superstructures that are based not only on linear but also on kinked and cyclic oligomers.[7] Nevertheless, research on molecular multicomponent architectures[8,9] and on patterns by pentagonal[10] or heptagonal molecules is still in its infancy. However, it is of fundamental relevance how the symmetry of molecules is translated into periodic patterns.[11]

Here we report the synthesis and patterns of shape-persistent macrocycles $[\mathbf{1}]_n$ ($n = 3-6$) based on condensed oligothiophene corner pieces linked via phenylene-ethynylene-butadiynylene (PEB) units (molecular models and chemical structures are shown in Figures 1 and 2, respectively).[12]

The macrocycles were prepared by Pd-catalyzed oxidative cyclooligomerization of the appropriate bisacetylenes.[13] Separation of the crude product by recycling gel permeation chromatography (recGPC) yielded the monodisperse compounds $[\mathbf{1}]_n$ ($n = 3-6$) (see Supporting Information). All macrocycles carry extraannular butyloxy chains at the heteropolycyclic corners and hexadecyloxy chains at the adaptable positions of the polygon sides, ensuring sufficient solubility of the target structures and the respective precursors. The molecules can be viewed as building blocks with symmetries D_{nh} ($n = 3-6$); however, the ring sizes and the alkoxy substituents guarantee a slight elastic deformability of the compounds ("soft polygons").

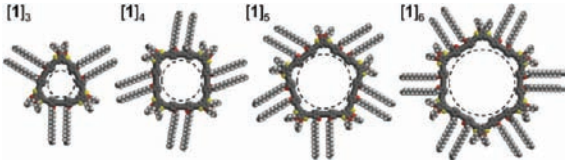

Figure 1. Molecular models of the cyclooligomers $[\mathbf{1}]_n$, $n = 3-6$. Maximum diameters of circles fitted into the cores: $[\mathbf{1}]_3$, 1.5 nm; $[\mathbf{1}]_4$, 2.4 nm; $[\mathbf{1}]_5$, 3.0 nm; $[\mathbf{1}]_6$, 3.8 nm.

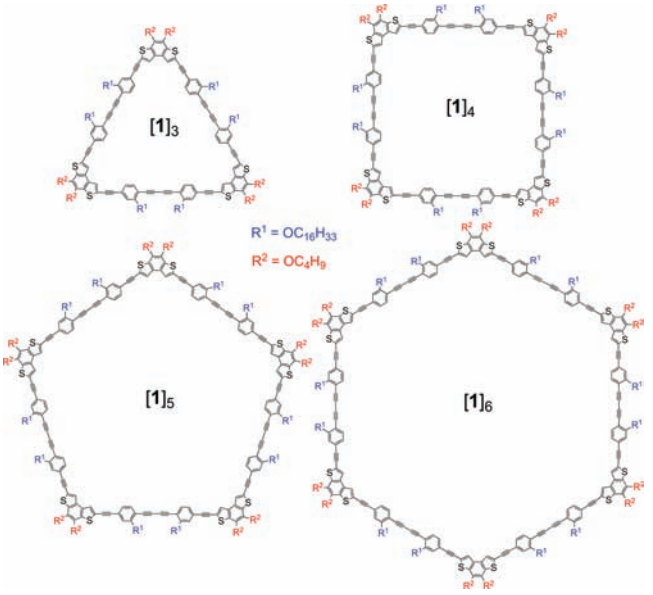

Figure 2. Molecular structures of the cyclooligomers $[\mathbf{1}]_n$, $n = 3-6$.

We investigated the molecular surface patterns of the pure compounds $[\mathbf{1}]_n$ and binary mixtures thereof by means of STM. The experiments were performed under ambient conditions at the interface of $10^{-4}-10^{-7}$ M solutions of the respective compound in TCB and HOPG. All macrocyclic oligomers assemble to highly ordered 2D patterns.

Trimers $[\mathbf{1}]_3$ form at low concentration (10^{-6} M, Figure 3a) a honeycomb network (*p6mm* symmetry)[14] where the macrocycle backbones (macrocyclic triangles) and interdigitating hexadecyloxy substituents define the corners and sides of the hexagonal

Received: April 18, 2011
Published: June 16, 2011

ACS Publications © 2011 American Chemical Society

dx.doi.org/10.1021/ja203536t | *J. Am. Chem. Soc.* 2011, 133, 11062–11065

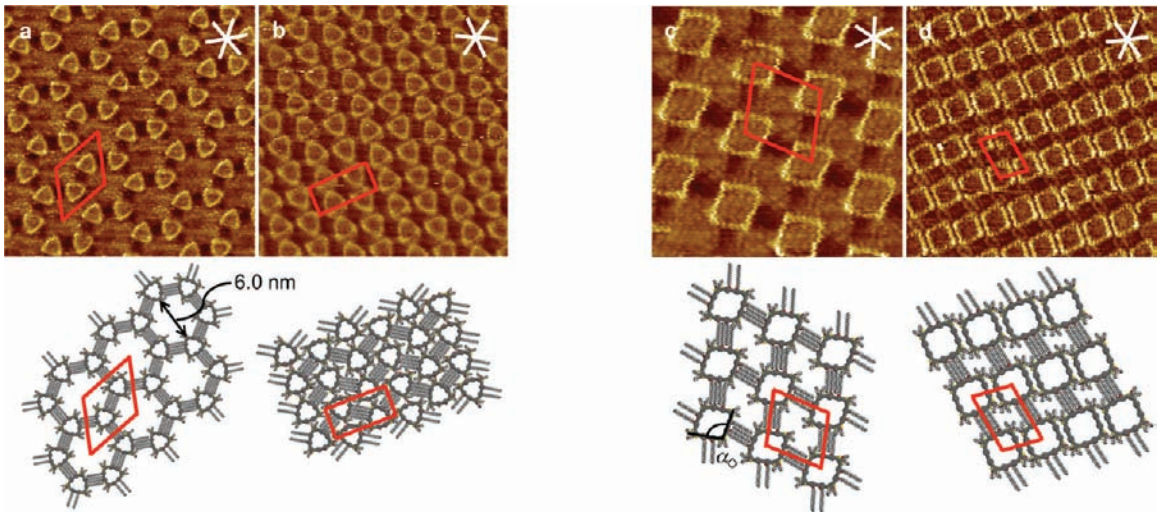

Figure 3. STM images and molecular models of the cyclooligomer patterns at the TCB/HOPG interface. (a), (b) $[\mathbf{1}]_3$ (a: $c = 10^{-6}$ M, 40.0 × 40.0 nm^2, $V_S = -1.0$ V, $I_t = 4$ pA, thermally annealed for 30 s at 60 °C; *p6mm*, $a = 8.2 \pm 0.2$ nm, $b = 8.1 \pm 0.2$ nm, $\gamma(a,b) = 60 \pm 2°$; b: $c = 10^{-5}$ M, 35.5 × 35.5 nm^2, $V_S = -1.0$ V, $I_t = 4$ pA, thermally annealed for 1 min at 60 °C; *p2mg*, $a = 7.8 \pm 0.2$ nm, $b = 3.7 \pm 0.1$ nm, $\gamma(a,b) = 90 \pm 2°$), and (c), (d) $[\mathbf{1}]_4$ (c: $c = 10^{-6}$ M, 29.5 × 29.5 nm^2, $V_S = -0.8$ V, $I_t = 30$ pA, thermally annealed for 1 min at 80 °C; *p2*, $a = 5.6 \pm 0.2$ nm, $b = 5.4 \pm 0.2$ nm, $\gamma(a,b) = 73 \pm 2°$; d: $c = 10^{-5}$ M, 34.9 × 34.9 nm^2, $V_S = -1.2$ V, $I_t = 10$ pA, thermally annealed for 1 min at 60 °C; *p2*, $a = 5.6 \pm 0.2$ nm, $b = 3.8 \pm 0.1$ nm, $\gamma(a,b) = 76 \pm 2°$). The unit cells are shown in red; the white lines indicate the HOPG main axis directions.[5]

intermolecular cavities with 6 nm diameter, respectively. In addition, the triangles provide interior pores with diameters of about 2 nm. The packing is supported by the 3-fold backbone symmetry, in accordance with the directions of the hexadecyloxy substituents, located at the adaptable positions of the triangle sides. They point outward to maximize the intermolecular linkages by an interdigitated alignment (along the HOPG main axis directions). At increased concentration (10^{-5} M, Figure 3b), a more dense packing results as an effect of higher adsorption degree.[6c] The macrocycles are assembled toward a crystal with mirror lines in one direction and glide mirror lines in the perpendicular direction to yield a *p2mg* plane group. Four hexadecyloxy substituents of two sides adsorb at the interface—intermolecularly interdigitated along two main axes of the substrate—while the other two chains point toward the solution phase or fill the inner ring cavity in a disordered fashion.

Tetramers $[\mathbf{1}]_4$ ($c = 10^{-6}$ M) assemble into an oblique pattern (Figure 3c) with *p*2 symmetry. All eight hexadecyloxy chains are extraannularly oriented and adsorbed along the substrate main axes with 60° alignment between the substituents of adjacent backbone sides. This leads to a distortion of the (predicted) quadratic backbone conformation ($\alpha_\diamond = 90°$) toward a rhombic shape ($\alpha_\diamond = 102 \pm 3°$). At increased concentration (10^{-5} M, Figure 3d), only four alkoxy substituents of two opposing sides of $[\mathbf{1}]_4$ adsorb onto the substrate, while the other four substituents are not imaged. The alkoxy chain commensurability with the underlying graphite allows in this case a (nearly) quadratic structure of the backbones. *p*2 symmetry is observed.[15]

Hexamers $[\mathbf{1}]_6$ at 2×10^{-6} M adsorb in an oblique nearly hexagonal packing (Figure 4a; *p6mm* plane group). The backbone geometries match the substrate symmetry, and all hexadecyloxy substituents point outward, interdigitate, are aligned along the HOPG main axes and stabilize a dense network. Trigonal and hexagonal pores are here defined as intermolecular and intramolecular cavities, respectively, inversely to $[\mathbf{1}]_3$, although of comparable size. At increased concentration, the backbones of $[\mathbf{1}]_6$ collapse toward a rectangular shape and assemble to a more

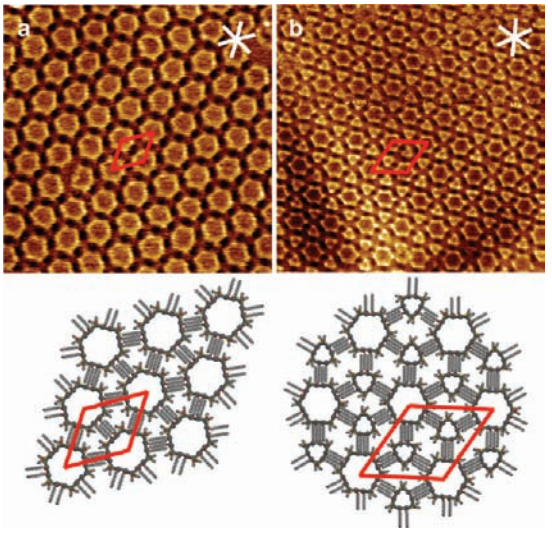

Figure 4. STM images and molecular models of the patterns of (a) $[\mathbf{1}]_6$ ($c = 2 \times 10^{-6}$ M, 62.8 × 62.8 nm^2, $V_S = -1.0$ V, $I_t = 6$ pA, thermally annealed for 1 min at 60 °C; *p6mm*, $a = 7.5 \pm 0.1$ nm, $b = 7.5 \pm 0.1$ nm, $\gamma(a,b) = 60 \pm 2°$) and (b) a binary mixture of $[\mathbf{1}]_3$ and $[\mathbf{1}]_6$ ($c([\mathbf{1}]_3) = 10^{-5}$ M; $c([\mathbf{1}]_6) = 10^{-7}$ M; $c([\mathbf{1}]_3)/c([\mathbf{1}]_6) = 100{:}1$; 79.9 × 79.9 nm^2, $V_S = -0.8$ V, $I_t = 9$ pA; *p6mm*, $a = 9.8 \pm 0.2$ nm, $b = 10.1 \pm 0.2$ nm, $\gamma(a,b) = 60 \pm 2°$) at the TCB/HOPG interface. The unit cells and substrate main axis directions are indicated in red and white color, respectively.[16]

dense packing, where the alkoxy substituents of two opposing sides interdigitate intermolecularly, and the remaining alkoxy substituents interdigitate within the cavity (see Supporting Information).

Shapes and sizes of the oligomers discussed above encouraged us to investigate binary mixed adlayers formed by macrocycles (polygons) which differ in the degree of oligomerization (corner or side numbers). In some cases only short-range adsorbate ordering (e.g., $[\mathbf{1}]_3$ and $[\mathbf{1}]_4$) is observed, or island structures of

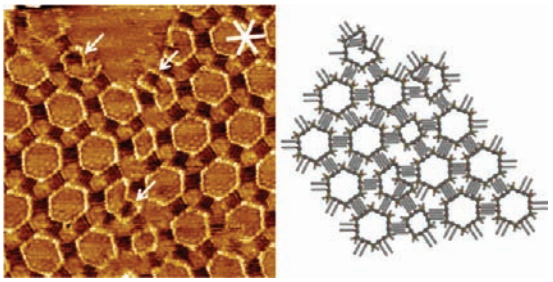

Figure 5. STM image and molecular model of a self-assembled monolayer of a mixture of $[\mathbf{1}]_4$ and $[\mathbf{1}]_6$ at the TCB/HOPG interface ($c([\mathbf{1}]_4) = c([\mathbf{1}]_6) = 7 \times 10^{-7}$ M, 37.2 × 37.2 nm^2, $V_S = -0.8$ V, $I_t = 5$ pA, thermally annealed for 30 s to 80 °C). The white lines indicate the HOPG main axis directions. Arrows indicate molecules $[\mathbf{1}]_6$ of a structure allowing intraannular alkoxy chain interdigitation (dark intraannular regions in the STM image).[5]

one compound are fenced by another macrocycle (e.g., $[\mathbf{1}]_6$ and $[\mathbf{1}]_5$) (see Supporting Information). However, $[\mathbf{1}]_3$ and $[\mathbf{1}]_6$ form spontaneously a mixed phase after applying a solution of 10^{-5} M $[\mathbf{1}]_3$ and 10^{-7} M $[\mathbf{1}]_6$ (100:1) to the HOPG substrate (Figure 4b). The interdigitation of the hexadecyloxy substituents and the shape complementarity of the trigonal backbone of $[\mathbf{1}]_3$ and the hexagonal backbone of $[\mathbf{1}]_6$ lead to a 2:1 mixed pattern of triangles and hexagons with a *p6mm* plane group, similar to the isolated compounds (cf. Figures 3a and 4a).[17] No triangle is (by the binding motif of interdigitating hexadecyloxy chains) connected to other triangles and no hexagon is connected to other hexagons — only heterogeneous neighboring occurs. Occasionally, also another phase of the mixed compounds $[\mathbf{1}]_3$ and $[\mathbf{1}]_6$ is observed, where the hexagonal porous structure of pure $[\mathbf{1}]_3$ is maintained (as seen in Figure 3a), and hexagons $[\mathbf{1}]_6$ intercalate randomly into some of the cavities (and no alkoxy substituents of $[\mathbf{1}]_6$ contribute to the packing, see Supporting Information).

The importance of the match of the components' symmetry for the formation of ordered coadsorbates becomes clear when a mixture of $[\mathbf{1}]_4$ and $[\mathbf{1}]_6$ is investigated. No long-range ordered pattern could be observed. Occasionally, $[\mathbf{1}]_4$ induces a lattice distortion in $[\mathbf{1}]_6$, leading in some cases even to a conformational flip (Figure 5). One corner of a hexagon turns inward, reduces the distances between sides aligned in parallel, and leads to an intraannular interdigitation of the alkoxy substituents.

With regard to the importance of the symmetry the pattern formation of the pentagons $[\mathbf{1}]_5$ is of special interest. 5-fold-symmetric molecules can not form crystalline tilings (i.e., densely packed patterns) on the Euclidean plane. However, recent work, for example, on corannulenes,[10] has displayed how nature generates structures with appropriate symmetry to resolve this problem. In the present case, it is neither clear if the pentagons form an ordered pattern at all, nor how the molecules achieve that.[17,18]

Figures 6a and b show that we are indeed able to observe two distinguishable long-range ordered patterns when solutions of pentamers $[\mathbf{1}]_5$ are brought into contact with the HOPG surface. At a concentration of 4×10^{-7} M, $[\mathbf{1}]_5$ forms porous structures with hexagonal symmetry, where six pentagons assemble around a central cavity into which the pentagon corners point (see Figure 6a, bottom). The 5-fold rotational symmetry (C_5) is lost after adsorption to the surface to yield a rotational symmetry C_1. The hexagonal assemblies form an oblique (not ideally hexagonal) overstructure. The crystal plane group is *p6*. Six

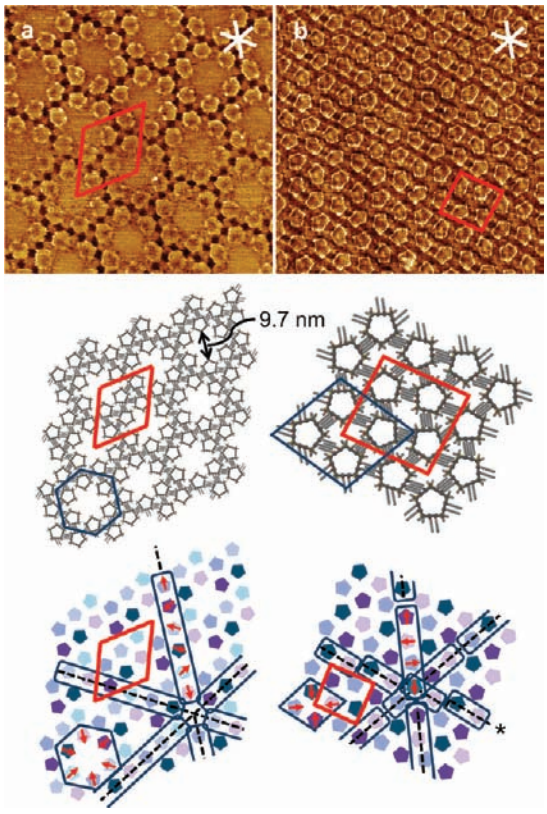

Figure 6. (a), (b) STM images and models of patterns of $[\mathbf{1}]_5$ at the TCB/HOPG interface (a: $c = 4 \times 10^{-7}$ M, 73.2 × 73.2 nm^2, $V_S = -1.0$ V, $I_t = 5$ pA, thermally annealed for 1 min at 80 °C; *p6*, $a = 19.6 \pm 0.5$ nm, $b = 19.3 \pm 0.5$ nm, $\gamma(a,b) = 61 \pm 2°$; b: $c = 10^{-6}$ M, 73.2 × 73.2 nm^2, $V_S = -0.6$ V, $I_t = 5$ pA, thermally annealed for 1 min at 80 °C; *p2*, $a = 12.7 \pm 0.2$ nm, $b = 12.6 \pm 0.2$ nm, $\gamma(a,b) = 89 \pm 2°$). In the molecular model shown in (a), only commensurably adsorbed hexadecyloxy substituents interdigitating with chains of adjacent molecules are shown. The unit cells are displayed in red, the repeating units are marked by the blue polygons, and the white lines indicate the HOPG main axis directions. In the schematic representations in the lower part, colors indicate different orientations of the pentagons. In (a), six different orientations occur to form a hexagonal repeating unit, while in (b) only four different orientations are observed and form the rhombic repeating unit. In (a) and (b), the linear rows (indicated by blue rectangular boxes) can be divided into hexuples and quadruples/dimers, respectively. Note: The idealistic molecular model in (b) involves equilateral pentagons, while the pentagons observed in the STM image are significantly distorted.

alkoxy substituents of three sides of each pentagon interdigitate with substituents of three pentagons of two neighboring hexagonal assemblies (and thus contribute to the packing), whereas the adaptable substituents of the remaining two sides point into the central cavity or toward the solvent and do not interdigitate. Not any two neighboring pentagons within such a hexagonal superstructure are directly linked by side chain interdigitation. They are always connected via a third (bridging) pentagon, assembled within a neighboring hexagonal superstructure. Alternatively, the packing can be described as parallel linear rows of macrocycles (following three directions with 60°/120° row-row angles), interrupted by a void on every seventh lattice site (see Supporting Information). Every molecule covers 55.2 nm^2 (as derived from the unit cell area divided by the number of molecules, here 6, per unit cell). If the concentration of pentagons $[\mathbf{1}]_5$ is increased to 10^{-6} M, a more dense packing

(40.0 nm^2 per molecule) is observed (Figure 6b). The repeating unit can be viewed as a rhombic assembly of four pentagons with corners pointing to the center (blue rhombus in Figure 6b, middle), and a nearly rectangular unit cell can be indexed. The molecules pack in a crystal with plane group *p*2. All five backbone sides of each pentagon contribute to the intermolecular interactions via interdigitating alkoxy substituents. As for the less dense packing, the molecules can be viewed as arranged in rows that are aligned along the three main symmetry axes of the HOPG. Along two directions, four pentagons $[\mathbf{1}]_5$ are connected via interdigitated side chains to form quasi-linear quadruples, discriminated by interrupts resulting from noncomplementary terminal pentagon corners of adjacent quadruples, pointing toward each other. Along the third direction, pentagons connected by interdigitated side chains assemble to a stepped straight line (* in Figure 6b), where each dimer of pentagons $[\mathbf{1}]_5$ is slightly translated in parallel. The orientations of the molecules in Figure 6a and b are not congruent with each other. The intercalation of a seventh molecule per unit cell in Figure 6a would decrease the required area to 47.3 nm^2 per molecule, still 18% larger than the average spatial requirement of each molecule in Figure 6b. Thus, the packing shown in Figure 6a cannot be transferred to the denser pattern (Figure 6b) without general reorientation of the molecules and changes of the intermolecular distances.

The investigation on $[\mathbf{1}]_5$ gave an insight into two principally different motives of the pattern formation of pentagons. As far as we know, this is the first adsorption study of "soft" pentagons on a solid substrate that unravels the question how these polygons can cover an HOPG surface.

In summary, we have shown that the oligomeric macrocycles behave as "molecular polygons" of different symmetries. Cyclooligomerization and separation of the crude product via recGPC has proven as an efficient method for the preparation of these molecules, which support the formation of molecular porous and dense long-range ordered patterns of complementary shapes. The results allow an efficient and deliberately predictable pattern design based on equilateral polygons and their mixtures with periodicities up to 19 nm. In addition, the elasticity of the "soft" molecule backbones and their flexible alkoxy fringe supports a crystallization of pentagons. All pattern dimensions are tunable not only by the alkoxy chain lengths (defining intermolecular distances), but also by the backbone diameters (defined by the length of the PEB rigid rod units and the corner building blocks). Current studies will cover that issue and in addition concentrate on the synthesis of nonsymmetrical macrocycles and the investigation of their patterns. Ultimately, design rules for classical (macroscopic) polygon tilings can be adapted to the supramolecular surface patterning by molecular building blocks.

■ ASSOCIATED CONTENT

Supporting Information. Additional STM images, experimental procedures and characterization for all new compounds. This material is available free of charge via the Internet at http://pubs.acs.org.

■ AUTHOR INFORMATION

Corresponding Author
hoeger@uni-bonn.de; stefan.jester@uni-bonn.de

■ ACKNOWLEDGMENT

Financial support by the DFG, the SFB 624, and the VolkswagenStiftung is gratefully acknowledged.

■ REFERENCES

(1) (a) De Feyter, S.; De Schryver, F. C. *Chem. Soc. Rev.* **2003**, *32*, 139. (b) Barth, J. V.; Costantini, G.; Kern, K. *Nature* **2005**, *437*, 671.

(2) Tahara, K.; Furukawa, S.; Uji-i, H.; Uchino, T.; Ichikawa, T.; Zhang, J.; Mamdouh, W.; Sonoda, M.; De Schryver, F. C.; De Feyter, S.; Tobe, Y. *J. Am. Chem. Soc.* **2006**, *128*, 16613.

(3) For SAMs of alkanes on HOPG see, for example: Yang, T.; Berber, S.; Liu, J.-F.; Miller, G. P.; Tománek, D. *J. Chem. Phys.* **2008**, *128*, 124709 and references therein.

(4) (a) Lazzaroni, R.; Calderone, A.; Brédas, J. L.; Rabe, J. P. *J. Chem. Phys.* **1997**, *107*, 99. (b) Sautet, P. *Chem. Rev.* **1997**, *97*, 1097.

(5) Confinement of TCB is observed for $[\mathbf{1}]_4$ and $[\mathbf{1}]_6$ (medium bright color encoding, Figures 3c and 5a; see Supporting Information).

(6) (a) Höger, S.; Bonrad, K.; Mourran, A.; Beginn, U.; Möller, M. *J. Am. Chem. Soc.* **2001**, *123*, 5651. (b) Tahara, K.; Johnson, C. A., II; Fujita, T.; Sonoda, M.; De Schryver, F. C.; De Feyter, S.; Haley, M. M.; Tobe, Y. *Langmuir* **2007**, *23*, 10190. (c) Lei, S.; Tahara, K.; De Schryver, F. C.; Van der Auweraer, M.; Tobe, Y.; De Feyter, S. *Angew. Chem.* **2008**, *120*, 3006. *Angew. Chem., Int. Ed.* **2008**, *47*, 2964.

(7) Jester, S.-S.; Shabelina, N.; Le Blanc, S. M.; Höger, S. *Angew. Chem.* **2010**, *122*, 6237; *Angew. Chem., Int. Ed.* **2010**, *49*, 6101.

(8) (a) Pan, G.-B.; Cheng, X.-H.; Höger, S.; Freyland, W. *J. Am. Chem. Soc.* **2006**, *128*, 4218. (b) Mena-Osteritz, E.; Bäuerle, P. *Adv. Mater.* **2006**, *18*, 447. (c) Chen, T.; Pan, G.-B.; Wettach, H.; Fritzsche, M.; Höger, S.; Wan, L.-J.; Yang, H.-B.; Northrop, B. H.; Stang, P. J. *J. Am. Chem. Soc.* **2010**, *132*, 1328.

(9) (a) Tahara, K.; Lei, S.; Mamdouh, W.; Yamaguchi, Y.; Ichikawa, T.; Uji-i, H.; Sonoda, M.; Hirose, K.; De Schryver, F.; De Feyter, S.; Tobe, Y. *J. Am. Chem. Soc.* **2008**, *130*, 6666. (b) Tahara, K.; Lei, S.; Mössinger, D.; Kozuma, H.; Inukai, K.; Van der Auweraer, M.; De Schryver, F. C.; Höger, S.; Tobe, Y.; De Feyter, S. *Chem. Commun.* **2008**, 3897. (c) Schmaltz, B.; Rouhanipour, A.; Räder, H. J.; Pisula, W.; Müllen, K. *Angew. Chem.* **2009**, *121*, 734. *Angew. Chem., Int. Ed.* **2009**, *48*, 720. (d) Adisoejoso, J.; Tahara, K.; Okuhata, S.; Lei, S.; Tobe, Y.; De Feyter, S. *Angew. Chem.* **2009**, *121*, 7489. *Angew. Chem., Int. Ed.* **2009**, *48*, 7353.

(10) (a) Merz, L.; Parschau, M.; Zoppi, L.; Baldridge, K. K.; Siegel, J. S.; Ernst, K.-H. *Angew. Chem.* **2009**, *121*, 2000. *Angew. Chem., Int. Ed.* **2009**, *48*, 1966. (b) Bauert, T.; Merz, L.; Bandera, D.; Parschau, M.; Siegel, J. S.; Ernst, K.-H. *J. Am. Chem. Soc.* **2009**, *131*, 3460. (c) Guillermet, O.; Niemi, E.; Nagarajan, S.; Bouju, X.; Martrou, D.; Gourdon, A.; Gauthier, S. *Angew. Chem.* **2009**, *121*, 2004. *Angew. Chem., Int. Ed.* **2009**, *48*, 1970.

(11) Plass, K. E.; Grzesiak, A. L.; Matzger, A. J. *Acc. Chem. Res.* **2007**, *40*, 287.

(12) The nomenclature describes cyclooligomers $[\mathbf{1}]_n$ with the cyclooligomerization degree *n*.

(13) (a) Glaser, C. *Ber. Dtsch. Chem. Ges.* **1869**, *2*, 422. (b) Siemsen, P.; Livingston, R. C.; Diederich, F. *Angew. Chem.* **2000**, *112*, 2740. *Angew. Chem., Int. Ed.* **2000**, *39*, 2632.

(14) Hahn, Th., Ed. *International Tables for Crystallography: Space Group Symmetry*, 5th ed.; Springer: New York, 2002.

(15) Additional patterns of $[\mathbf{1}]_4$ are described in the Supporting Information.

(16) The requirement of the concentration ratio $c([\mathbf{1}]_3):c([\mathbf{1}]_6)$ = 100:1 originates from different adsorption efficiencies and has been reported before (cf. ref 9d). In other words, $[\mathbf{1}]_6$ adsorbs much more effectively than $[\mathbf{1}]_3$.

(17) Grünbaum, B.; Shephard, G. C. *Tilings and Patterns*; Freeman: New York, 1987; pp 57−112.

(18) Schilling, T.; Pronk, S.; Mulder, B.; Frenkel, D. *Phys. Rev. E* **2005**, *71*, 036138.